BEHAVIORAL STUDY OF RAYLEIGH, LAMB, AND CRITICALLY REFRACTED LONGITUDINAL WAVES FOR CRACK DETECTION IN PAINTED AND RUSTED STEEL STRUCTURAL COMPONENTS

Reynold Franklin[1] and Udaya B. Halabe[2]

[1] Executive Vice President, Stueve Construction Co., 2201 East Oak Street, Algona, IA, 50511, USA;
E-mail: RFranklin@stueve.com

[2] Professor, West Virginia University, Department of Civil and Environmental Engineering,
Morgantown, WV 26506-6103, U.S.A.
E-mail: Udaya.Halabe@mail.wvu.edu

Corresponding Author
Dr. Udaya B. Halabe
Professor, West Virginia University,
Department of Civil and Environmental Engineering,
P.O. Box 6103, Morgantown, WV 26506-6103,
U.S.A.
E-mail: Udaya.Halabe@mail.wvu.edu

ABSTRACT

This paper presents the results of an experimental study performed to understand the behavior of various refracted ultrasonic waves in steel structural components. A comparative study was conducted using critically refracted longitudinal waves, symmetrical and unsymmetrical Lamb waves, and Rayleigh waves. The influence of surface paint and rust on these waves and the impact on fatigue crack detection has beendiscussed. Time and frequency domain analyses were used to detect fatigue cracks and the distinct advantage of spectral analysis over time domain analysis is reported. Symmetrical and unsymmetrical Lamb waves and critically refracted longitudinal waves showed less promise for crack detection when compared to Rayleigh waves. One interesting observation was that ultrasonic waves tend to propagate through the paint in a crack rather than around the crack. Another important observation was the change in group velocity of Lamb waves on coated plates. Although generally successful in detecting the presence of crack in uncoated and rusted specimens, there were serious difficulties in obtaining signals in the pulse echo mode in case of Lamb waves for the painted specimens. Therefore, Rayleigh waves are recommended for crack detection in steel members under uncoated, painted, or rusted condition since these waves are highly sensitive to surface cracks.

Keywords: Cracks, Crack Detection, Rayleigh Waves, Lamb Waves, Steel, Rusted Steel, Painted Steel, Ultrasonics.

1. INTRODUCTION

Application of ultrasonic testing for damage detection and condition assessment of infrastructure has been the focus of many past studies [1-25]. In this aspect, detection and classification of fatigue cracks that originate on the surface of steel structural members is very important. Rayleigh and Lamb waves have been successfully used to detect fatigue cracks in uncoated metallic members [1-9]. However, field implementation of ultrasonic technique for steel structural members has been greatly hindered by the presence of rust and paint.Significant cost is involved in removal of paint and rust and repainting the member. Detection of fatigue cracks that initiate on the surface of steel structural members is influenced by paint and rust. The effect of surface coating on the ultrasonic waves and its implication on fatigue crack detection has to be clearly understood for successful field implementation. This paper presents a comparative study of various types of refracted ultrasonic waves and the influence of surface coating on the ability of these waves to detect cracks in steel members. Use of Rayleigh waves, symmetrical Lamb waves, unsymmetrical Lamb waves, and critically refracted Longitudinal (L_{CR}) waves were evaluated in this study.

Rayleigh waves have been very effective in detecting fatigue cracks in uncoated specimens. Several researchers have used these waves to detect fatigue cracks [7,9-15,18,22]. Some researchers have demonstrated the effect of surface roughness on Rayleigh waves[21]. Some success on sizing of cracks using Rayleigh waves has also been reported [18]. Lamb waves have also shown success in detecting fatigue cracks and have especially been studied for use in long steel members [4,17,24,25]. Lamb waves have also been used to detect corrosion in pipes which is an indication that these waves are also influenced by surface conditions [1,2,3]. Critically refracted longitudinal waves have been used for some interesting applications [6,8,16]. These waves have the ability to skim under the surface and are not likely to be influenced by surface conditions. However, their ability to detect fatigue cracks has not been fully explored. Several researchers have emphasized the need for spectral analysis to enhance the sensitivity and reliability of ultrasonic testing for crack detection [11-15,22,23]. This study also uses time and frequency domain parameters to detect fatigue cracks with emphasis on painted and rusted steel specimens.

2. EXPERIMENTAL STUDY

2.1 Measurement Conditions and Test Specimens

Angle-beam ultrasonic contact transducer with polystyrene wedges (with different incident angles) were used to produce the different types of waves used in this study. The central frequency of the longitudinal (P-wave) transducer was 1 MHz with a fairly narrow bandwidth of 0.4 MHz (0.8 MHz to 1.2 MHz at - 6dB). Such narrow bandwidth transducers are expected to produce well-defined refracted waves. The P-wave transducer was attached to polystyrene wedges (with different incident angles) to generate different types of waves (e.g., Rayleigh waves, Lamb waves, critically refracted longitudinal waves) in the steel specimen. The wedge angle adopted to produce Rayleigh waves was 52^o, which was slightly higher than the second critical angle of 46^o corresponding to critically refracted shear waves. Refracted Lamb waves were produced in the region where the dispersion of these waves was minimum. The dispersive nature of Lamb waves and the approach to produce non-dispersive Lamb waves using contact transducers is available in published references [2,5]. The wedge angles used were 23^o to obtain symmetrical Lamb waves in mode L_{13} and 46^o wedges for unsymmetrical Lamb waves of mode L_{21}. Critically refracted longitudinal waves (L_{CR} waves) are also produced around the first critical angle of 23^o. While the wedge angles for critically refracted longitudinal waves and symmetrical Lamb waves are identical, depending upon the plate thickness and the frequency of excitation only one of these refracted waves will be generated.A high powered sine wave pulser was used to excite the transducers. The signals were received using a broadband receiver. A digital oscilloscope was used to acquire and digitize the signals. The maximum

receiver gain without any signal saturation was adopted for each wave type and is reported in their corresponding sections. The digitization rated adopted for this study was 10 MHz. The effect of random noise was minimized by averaging 100 waveforms. Kaiser bandpass digital filter in the range of 0.8 MHz to 1.2 MHz was used to remove frequency dependent noise. A window of 1024 points was extracted from the received signal for analysis. Two broken lines in the later figures show the extracted window. A digital signal processing software was used for analyzing the signals in the frequency domain. Signal amplitude and energy are influenced by the variations in contact between the material and the transducer. Preliminary studies indicated that when Ultraagel-II couplant was used on the wedge-material interface, high energy and amplitude signals were produced. In addition this couplant has corrosion inhibitor property and is best suited for the wedge-material interface. Sonoglide couplant was used in the senor-wedge interface because of its very long drying time and excellent transducer lubricant properties, in addition to producing excellent amplitude and energy signals. Also, optimal clamping force for each wedge was obtained based on high signal energy and repeatability of obtaining them in the laboratory [10].

Steel plates of size $2200 \times 76 \times 6.8$ mm were used in this study to obtain the behavior of Rayleigh and Lamb waves. These plates simulated the flanges of steel I-beams. One steel plate had a machined surface cut (25 mm long, 0.7 mm wide, and 1.5 mm deep) simulating the fatigue crack. A different plate thickness was required for L_{CR} waves to avoid generation of Lamb waves. Behavior of L_{CR} waves were studied on a steel plate $2200 \times 76 \times 38$ mm. All the plates were tested using ultrasonic waves in direct-transmission andpulse-echo modes. The transducers were positioned such that the travel distances were 2 m in direct-transmission and 4 m in pulse-echo. The transducers were excited with five-cycle sine pulse of 400 volts peak-to-peak for pulse-echo transmission to produce narrow echo signals and ten cycle sine pulse of 400 volts peak-to-peak for direct-transmission tests to produce strong signals by exciting the transmitting transducer at resonance for a greater time. The plates were tested first without any surface coating on them. Secondly, the plates were tested with paint coating on them. The paint coating consisted of three layers, first layer of Low V.O.C. (Volatile Organic Compounds) Inorganic Zinc Primer P-139, second layer of Water Guard Intermediate/Primer W-112, and the third layer of Water-Guard Gloss Finish W-177. These paints are used by the highway departments in a number of south-eastern states in the U.S.A. including the states of Virginia, West Virginia, Maryland, North Carolina, South Carolina, and New Mexico. P-139 is a two component low V.O.C. inorganic zinc rich primer, which provides cathodic protection for ferrous metals. W-112 is an acrylic water-based paint free from lead and chrome. This product is designed for protection of ferrous, aluminum and galvanized metal surfaces. W-177 is an acrylic-based lead and chrome free gloss finish paint for heavy-duty protection and is specifically designed for metal protection. The total thickness of the paint coating ranged between 0.22 mm to 0.27 mm and had an average thickness of about 0.25 mm. Finally, the plates were tested under surface rust condition. For generating surface rust in the plate, all paint was removed from the steel plates using commercial paint remover. Surface rust was induced in the steel plates by exposing them to moisture and high humidity for several weeks. The following sections describe the behavior of the various ultrasonic waves under the different surface coating.

2.2 Behavior of Rayleigh Waves

Pulse-echo signals were received using a constant receiver gain of +8 dB which enabled the study of the impact of surface coatings. The optimal clamping force used on the wedges was 40 lb. The signal obtained in uncoated condition showed a strong crack echo. In case of painted condition, the signal could not be obtained with paint under the transducer. Hence, paint was removed in the area under the transducer to obtain the signal shown in Figure 1. Although this was a low amplitude signal, the presence of crack could easily be seen from the crack echo. Figure 2 shows the signal obtained from the rusted specimen. The signal clearly shows the presence

of the crack. The presence of crack was also located from direct-transmission signals. The experimental results obtained from using Rayleigh waves in pulse-echo and direct-transmission is shown in Table 1.

In pulse echo mode, the presence of a crack echo and subsequent loss in backwall echo amplitude clearly showed the presence of crack. Presence of the crack is also seen from spectral analysis of the backwall echo. Drop in magnitude, area, and third moment of the Power Spectral Density (PSD) curve corresponding to backwall echo was more than 50% due to the presence of crack. No significant change was observed in the central frequency of the signals. Direct transmission signals were received at a constant gain of 0 dB. Presence of crack was identified from the arrival time, amplitude and energy in the signal. The crack caused a delay of 5 to 10 μs in the arrival time for the direct transmission mode. The loss in the PSD curve parameters such as the peak magnitude, area, and third moment was around 60%. However, when there was paint coating the energy loss due to the crack was more than 90%. No appreciable change was observed in the central frequency of the signals. A simple test was conducted to understand why there was a greater energy loss in painted sections. Direct transmission test was performed on a 0.50 m long steel plate with 20 mm long crack across the width. Signals were acquired from the cracked section with and without paint inside the crack. The signal energy dropped from 0.24 V^2Hz to 0.16 V^2Hz due to the presence of paint in the crack. This illustrates that the presence of paint in micro cracks causes the ultrasonic waves to travel through the paint rather than around the crack, which results in significant energy loss due the attenuation caused by the paint.

The study showed a significant decrease in signal amplitude and energy due to the presence of paint in pulse echo and direct transmission modes. The impact was lot less due to presence of rust. Significant change was also noticed in the arrival time of the signals due to the presence of surface conditions. This impact translated to a 4% error in locating the cracks from the pulse echo signals. Nevertheless, the experimental results do show that Rayleigh waves can be successfully used to detect and locate cracks even under surface coatings such as paint and rust provided the surface under the transducer is cleaned and free from paint.

2.3 Behavior of Symmetrical Lamb Waves

The effect of surface coatings on Lamb waves and their impact on crack detection was studied using Lamb waves generated by narrow and broad wedges. Narrow wedges produce much stronger signals which is seen by comparing Figures 3 and 4. Figure 3 and 4 are the signals received from the uncoated cracked plate using the broad and narrow wedges respectively. The constant clamping force on the broad wedges were 40 lb and on the narrow wedges were 20 lb. Constant gain of 24 dB for the narrow wedges and 40 dB for the broad wedges was used to acquire the pulse echo signals.Despite the lower gains used to receive the signal, narrow wedges produced stronger and better echoes in the pulse echo signals. The test results are shown in Tables 2 and 3. The sharpness of the crack echo is very good in Figure 4 whereas in Figure 3 where no clear crack echo is seen. In case of Figure 3, the presence of crack could be seen only form spectral analysis of the backwall echo. Decrease in magnitude, area, and third moment of the PSD curve was more than 50% due to the crack in the uncoated and the rusted plates. No appreciable change in central frequency was obtained. Moreover, the presence of surface rust did not significantly reduce the signal strength unlike the case of Rayleigh waves. However, when paint coating was present on the plate,very low amplitude backwall echo was observed from the uncracked section in the pulse echo mode. From the cracked section, neither backwall nor cracked echo was observed. This prevented further analysis and no comparison could be made. Unlike Rayleigh waves, symmetrical Lamb waves showed no improvement in the signal with the removal of paint under the transducer. This behavior was observed even for the strong signals generated using the narrow wedges.

Direct transmission testing was also performed using symmetrical Lamb waves and the results are also shown in Tables 2 and 3. The crack caused a delay of about 1 to 3μs in the arrival time. For cases of no coating

or rust the drop in area and third moment was around 10% due to the presence of crack for broad wedges and 20% for narrow wedges. However when paint was present, the same parameters showed a 90% or higher drop between uncracked and cracked cases. This is because of the tendency for the waves to travel through the paint rather than around the crack, which could result in greater attenuation and possibly change in modes of the Lamb waves. The signals received from the uncracked and cracked sections under rusted condition are shown in Figures 5 and 6. Their corresponding PSD curves are shown in Figure 7 where the cracked section produced a higher magnitude compared to the uncracked section indicating Peak Magnitude of PSD curve would not be a very reliable parameter for crack detection. However,the cumulative area plots shown in Figure 8indicate a drop in signal energy corresponding to the cracked section.

Changes in arrival time between the uncoated and painted specimens indicate the change in group velocity. This suggests that symmetrical Lamb waves traveled in the painted plate like in a composite plate, with an upper thin layer of paint and lower steel plate.

Signals produced by narrow wedges were much stronger than signals generated using broad wedges. Nevertheless, the behavior of both waves were identical in terms of the presence of crack and surface conditions.In pulse echo mode, removing the paint under the transducer did not result in improved signals. The experimental study showed that rust had much lower effect on the signal strength in case of Lamb waves compared to Rayleigh waves. However, symmetrical Lamb waves (mode L_{13}) were greatly influenced by the presence of paint. This was inferred by the large loss in direct transmission signal amplitude and energy as well as the delayed arrival time. Moreover, pulse echo signals could not be obtained from painted sections.Since the generation of Lamb waves is dependent on the member thickness, and pulse echo signals could not be obtained from painted specimens, this technique offers less promise for crack detection compared to using Rayleigh waves.

2.4 Behavior of Unsymmetrical Lamb Waves

Unsymmetrical Lamb waves in mode L_{21} was used in this study. Pulse echo signals were received with a constant receiver gain of 52 dB. The signal received from the rusted specimen with crack is shown in Figure 9. The test results obtained for the various conditions are shown in Table 4. Crack and backwall echoes were present for the uncoated and rusted condition. However, for painted condition, no waveforms were obtained in the pulse echo mode. Even removal of paint under the transducer did not help in obtaining a signal. Hence no analysis could be performed for the painted condition. For the uncoated and rusted condition, presence of crack was seen from the crack echo and spectral analysis of the backwall echo. Decrease in magnitude, area, and third moment of the PSD curve was about 30 to 50% for the uncoated case, and more than 60% for the rusted case due to the presence of crack. No significant change was observed in the central frequency. The position of the crack obtained from the crack echo was very precise.

Direct transmission signals using unsymmetrical Lamb waves were received at a constant gain of 32 dB. The obtained test results are also shown in Table 4. The crack caused a small delay of about 4 to 6 μs in the arrival time of the signals. The presence of crack was clearly observed in the spectral analysis results for the various conditions. Decrease in peak magnitude, area, and third moment was about 10% or less due to the presence of the crack. When painted, the same parameters showed a drop of more than 90%. Obtaining signals from painted section was very difficult. Removing paint under the transducer did help a little. In case of the rusted specimen, the decrease in signal energy was about 50% which is much higher than in case of symmetrical Lamb waves, but comparable to the drop seen in case of Rayleigh waves. The central frequency did not show any change due to the presence of the crack. Like symmetrical Lamb waves, unsymmetrical Lamb waves also tend to travel in painted specimens as a composite plate as noticed by the decrease in the group velocity.

2.5 Behavior of Critically Refracted Longitudinal Waves

Pulse echo signals were received forL_{CR}waves using a constant gain of 36 dB. The pulse echo signals obtained for the uncoated condition from the cracked section is shown in Figure 10. The time domain signals did not show any crack echo for the uncoated or any of the coating conditions. However, spectral analysis did show significant loss in the signal parameters as shown in Table 5. The peak magnitude, area, and third moment of the PSD curve showed a decrease of about 50% corresponding to the crack. No change was observed in the central frequency of the signals.

Direct transmission signals were received using L_{CR} waves at a constant gain of 32 dB. The obtained results are shown in Table 5. The presence of paint coating in the steel plate did influence the signal and caused a 50% drop in the energy. Removing paint under the transducer helped get a better signal, but the decrease was still 40%. Rusted plate showed a 30% decrease in the signal energy. Under each surface condition, differences in signals were observed when ultrasonic waves encountered a crack. Although very little change was seen in the arrival time, the spectral parameters show significant differences between the uncracked and cracked cases. The area and third moment of the PSD curve decreased by about 45% for the uncoated condition. Peak magnitude also showed a decrease but the central frequency did not change. Similar results were also obtained for the rusted condition. However, for painted condition the drop in signal between the cracked and uncracked section was only about 20%, indicating lessersensitivity for crack detection.

Based on the test results, L_{CR} could be used to detect cracks using the spectral analysis, since time domain parameters are not very reliable. However, the detection will not be complete because location of the crack cannot be determined due to the absence of crack echo (Figure 10). The L_{CR} waves produced a very long wavetrain, which did not have a clearly defined end. Hence the extracted window for spectral analysis had to be confined to a defined time zone rather than the echo region. Also, several spurious signals (possibly refracted shear waves) were observed. However, since these spurious signal echoes were arriving at a later time it was easy to avoid these echoes in the signal analysis. As far as the presence of surface coating such as paint and rust, critically refracted longitudinal waves were not affected as much as Rayleigh and Lamb waves.

2.6 Attenuation Study

Attenuation characteristics of the various types of ultrasonic waves were also studied using spectral analysis. Direct transmission signals were received from steel plates under uncoated and painted conditions. The receiver gain was kept at a 0 dB to compare the strength of each signal. Appropriate ultrasonic couplant and clamping forces were also used. Signals were received from four travel distances 0.25 m, 0.50 m, 0.75 m, and 1.00 m. In case of L_{CR} waves 0.50 m, 0.75 m, 1.00 m, and 1.25 m were adopted because at 0.25 m distance, creeping longitudinal waves were also received which was evident from the high energy received at this distance. Since attenuation is frequency dependent, the received signals were passed through Kaiser bandpassfilters between 0.8 MHz and 1.2 MHz. Spectral analysis was performed on an extracted window of 1024 points and the area under the PSD curve (which is a representation of the signal energy) was used to determine the attenuation coefficient for the waves. The relationship between the signal energy(E) and total attenuation(α) is

$\ln(E) = \ln(E_o) - 2\alpha x$

Linear regression analysis was performed between ln(E) of the received signal and the various travel distance(x), which resulted in the values shown in Table 6. The initial energy(E_o) or y-intercept and the attenuation coefficients obtained from the regression analysis show the behavior of the ultrasonic waves. The increase in the attenuation coefficient due to the presence of paint was about 20% for the Rayleigh waves, 30% for Lamb waves and 5% for the L_{CR} waves. Although the attenuation coefficient value for Rayleigh waves was higher compared to the other waves, its initial energy(E_o) is also much higher compared to the other waves which indicates its

ability to travel greater distances. This explains why signals could be obtained in pulse echo modes from the painted specimen using Rayleigh waves and not by Lamb waves. The very small change seen in the attenuation coefficient of the L_{CR} waves between unpainted and painted conditions indicates the very little impact painted surface could have on the propagation of these waves. The high values of coefficient of determination, R^2, obtained from the regression analysis indicates the effectiveness of spectral analysis in obtaining the attenuation coefficients.

3. CONCLUSIONS

Refracted ultrasonic waves such as Rayleigh waves, Symmetrical Lamb waves, Unsymmetrical Lamb waves and Critically Refracted Longitudinal waves, could detect the presence of cracks in direct transmission mode but pulse echo mode was a failure for all but Rayleigh waves. The presence of cracks was primarily detected based on the decrease observed in the PSD curve parameters such as magnitude, area, and third moment. However, peak magnitude of the PSD curve is not a very reliable parameter as seen in case of symmetrical Lamb waves for the rusted condition. The presence of crack did not change the central frequency of the PSD curve significantly, hence, the behavior of the area and third moment parameters were almost identical. Very small changes were observed in the arrival time and amplitude in the time domain due to presence of a crack, hence it is important to use the spectral parameters such as area or third moment. Rayleigh waves produced very distinctive echo signals for the uncoated, painted and rusted conditions. Presence of paint in the crack caused the wave to travel through the paint in the crack rather than around the crack, which is different from the wave propagation behavior in uncoated specimens. This caused a significant energy loss in painted specimens with cracks. Symmetrical and Unsymmetrical Lamb waves were less sensitive to surface cracks and no pulse echo signals could be obtained from the painted specimens. On painted specimens, the Lamb wavepropagation is similar to that in a composite plate, with an upper thin paint layer and lower steel plate. L_{CR} waves did not produce any clear crack echoes and had no definitive end to the received wavetrain. Moreover, other spurious echoes were also seen in the signal. Hence, L_{CR} waves are not promising for crack detection.

The presence of paint coating significantly reduced the signal amplitude and energy for allwave types. Rusted plate also showed loss in signal amplitude and energy. L_{CR} waves were the least affected while Rayleigh and Lamb waves were highly affected due to the presence of surface coating. Removal of paint from the area under the ultrasonic transducers helped obtain better signals, especially in the case of Rayleigh waves. Attenuation study shows that although Rayleigh waves are the most affected by paint, much stronger signals could also be generated compared to the other waves. Based on the comparative study, Rayleigh waves are recommended for fatigue crack detection in uncoated, painted, or rusted steel specimens.

REFERENCES

1. Alleyne, D. N., and Cawley, P. (1997). “Long range propagation of Lamb waves in chemical plant pipework,” *Materials Evaluation*, **55**(4), 504-508.
2. Alleyne, D. N., and Cawley, P. (1996). “The excitation of Lamb waves in pipes using dry-coupled piezoelectric transducers,” *Journal of Nondestructive Evaluation*, **15**(1), 11-20.
3. Alleyne, D. N., and Cawley, P. (1995). “The long range detection of corrosion in pipes using Lamb waves,” *Review of Progress in Quantitative Nondestructive Evaluation*, Snowmass Village, Colorado, **14B**, 2073-2080.
4. Alleyne, D. N., Pialucha, T. P., andCawley, P. (1993). “A signal regeneration technique for long-range propagation of dispersive Lamb waves,” *Ultrasonics*, **31**(3), 201-205.
5. Alleyne, D. N., and Cawley, P. (1992). “Optimization of Lamb wave inspection techniques,” *NDT& E*

International, **25**(1), 11-21.

6. Bray, D. E., and Junghans, P. (1995). "Application of the LCR Ultrasonic technique for evaluating of post-weld heat treatment in steel plates," *NDT&E International*, **28**(4), 235-242.
7. Deutsch, W. A. K., Cheng, A., and Achenbach, J. D. (1997). "Self-focusing surface wave array," *Review of Progress in Quantitative Nondestructive Evaluation*, **16B**, 2077-2084.
8. Dickens, J. R., Bray, D. E., and Bender, D. A. (1996). "Beam profiles in wood from critically refracted longitudinal wave probes," *Materials Evaluation*, **55**(6), 721-725.
9. Dymkin, G. Ya., and Maksimov, A. V. (1988). "Reflection of Rayleigh waves from subsurface defects," *Russian Ultrasonics*, **18**(4), 203-205.
10. Franklin, R. (1998). "Innovative ultrasonic methodology for fatigue crack detection in steel members," *Ph.D. Dissertation*, West Virginia University, Morgantown, West Virginia, USA.
11. Halabe, U. B., and Franklin, R. (2013). "Detection of cracks in long painted or rusted steel beams using ultrasonic Rayleigh waves," *European International Journal of Science and Technology (EIJST)*, **2**(7), 161-182.
12. Halabe, U. B., and Franklin, R. (2001). "Fatigue crack detection in metallic members using ultrasonic Rayleigh waves with time and frequency analyses," *Materials Evaluation*, **59**(3), 424-431.
13. Halabe, U. B., and Franklin, R. (1999). "Detection of flaws in structural members using spectral analysis of ultrasonic signals," *Nondestructive Testing and Evaluation*, **15**(3/4), 215-236.
14. Halabe, U. B., and Franklin, R. (1998). "Ultrasonic signal amplitude measurement and analysis techniques for nondestructive evaluation of structural members," *Proceedings of SPIE Conference-Nondestructive Evaluation of Materials and Composites II*, San Antonio, Texas, **3396**, 84-94.
15. Halabe, U. B., and Franklin, R. (1997). "Crack detection in metallic structural members using ultrasonic technique," *ASNT Spring Conference and Sixth Annual Research Symposium*, Houston, Texas, 36-38.
16. Junghans, P. G., and Bray, D. E. (1991). "Beam characteristics of high angle longitudinal wave probes," *NDE Applications, Advanced Methods, and Codes, and Standards*, *ASME*, 216/NDE-9, 39-44.
17. Komsky, I. N., and Achenbach, J. D. (1992). "A self-calibrating ultrasonic technique for nondestructive inspection of airplane structures," *1992 ASNT Fall Conference and Quality Testing Show*, Chicago, Illinois, 58-61.
18. Lamy, C. A., Rebello, J. M. A., and Charlier, J. (1996). "Sizing of inclined surface flaw by the time-of-flight technique," *Proceedings of the 14th World Conference on NDT*, New Delhi, India, **4**, 2345-2348.
19. Masserey, B. (2006). "Ultrasonic surface crack characterization using Rayleigh waves,"Dissertation submitted to the Swiss Federal Institute of Technology Zurich for the degree of Doctor of Technical Sciences, Zurich, Switzerland, 1-151.
20. Palmer, S. B., Dixon, S., Edwards, R. S., and Jian, X. (2005). "Transverse and longitudinal crack detection in the head of rail tracks using Rayleigh wave-like wideband guided ultrasonic waves,"*Nondestructive Evaluation and Health Monitoring of Aerospace Materials, Composites and Civil Infrastructure IV, Proceedings of SPIE*, Bellingham, WA, **5767**, 70-80.
21. Planichamy, A., and Jayakumar, T. (1996). "Grain size measurements by ultrasonic Rayleigh surface waves," *Proceedings of the 14th World Conference on NDT*, New Delhi, India,**4**, 2253-2256.
22. Shyu, H. F. And Lock, M. W. B. (1996). "Ultrasonic testing system with split spectrum processing for HAZ creep evaluation," *Proceedings of the 14th World Conference on NDT,* New Delhi, India, **4**, 2105-2108.
23. Sinclair, A. (1985). "Analysis of the ultrasonic frequency response for flaw detection: A Technical Review," *Materials Evaluation*, **43**, January, 105-107.

24. Woodward, C., White, K. R., Reyes, G., and Parashis, A. (1996a). "Long range fatigue crack detection in steel bridge girders," *Proceedings of the 3rd Conference of Nondestructive Evaluation of Civil Structures and Materials*, Boulder, Colorado, 101-107.

25. Woodward, C., White, K. R., Parashis, A., and Carrica, V. (1996b). "Ultrasonic evaluation of steel bridge girders over long ranges," *Proceedings of Structural Materials Technology*, San Deigo, California, 34-39.

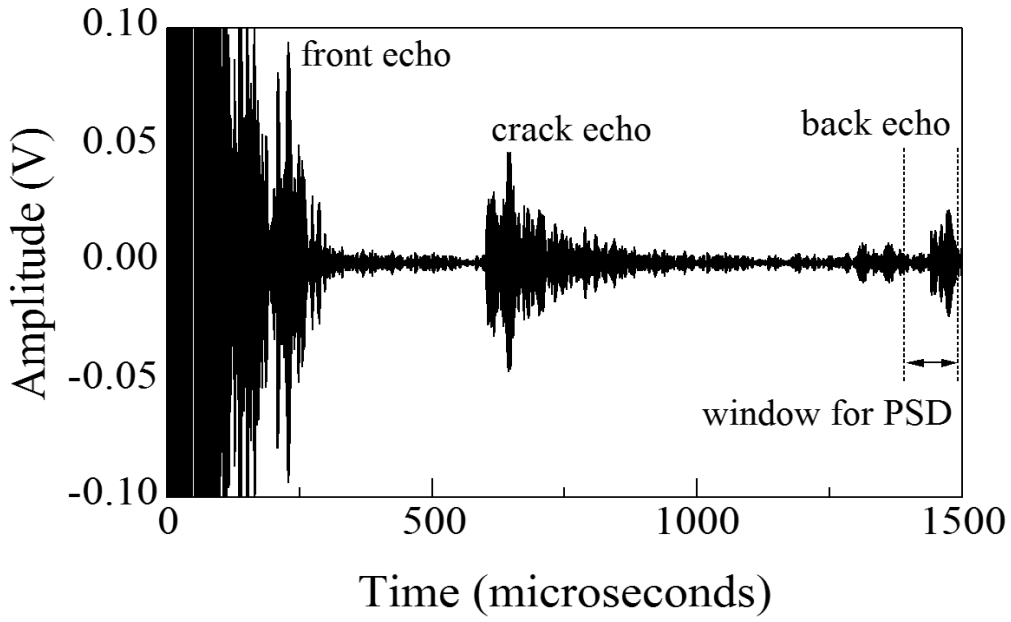

Figure 1. Pulse-Echo Signals Obtained Using Rayleigh Waves from Painted Plate

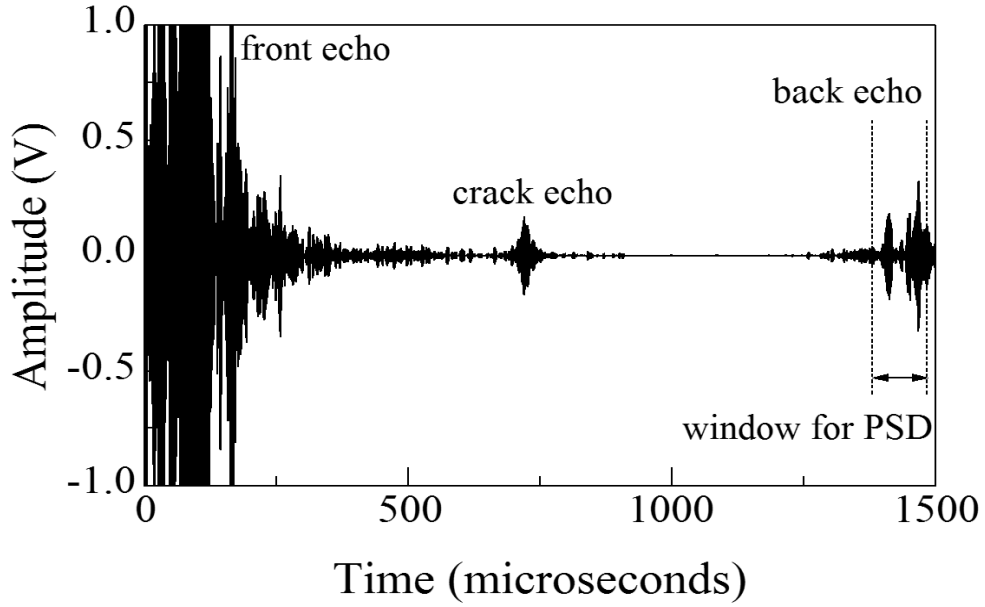

Figure 2. Pulse-Echo Signals Obtained Using Rayleigh Waves from Rusted Plate

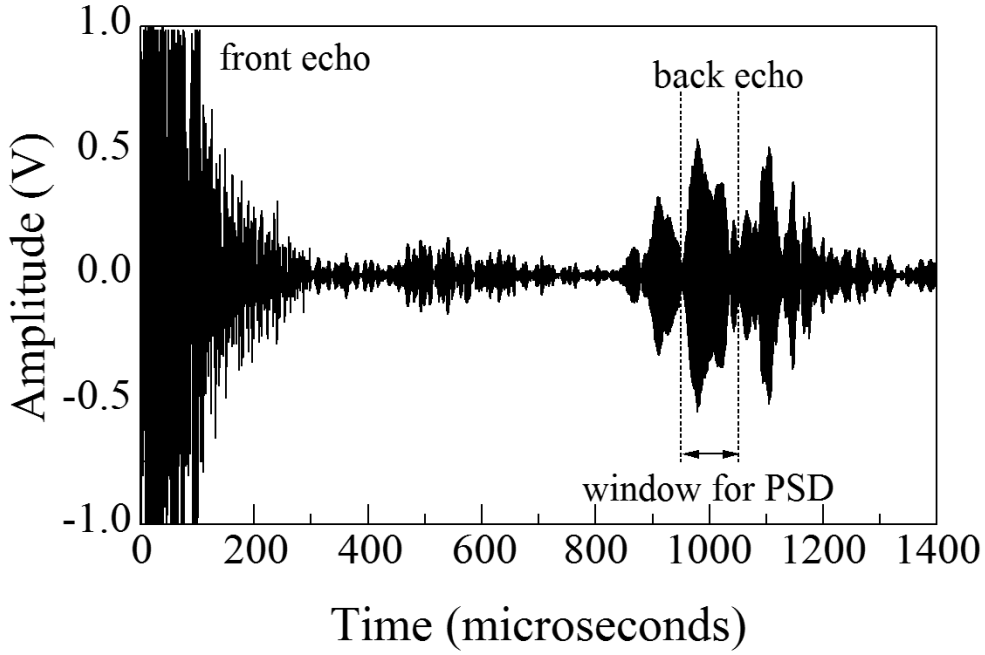

Figure 3. Pulse-Echo Signals Obtained Using Symmetrical Lamb Waves (Broad Wedge) from Uncoated Plate

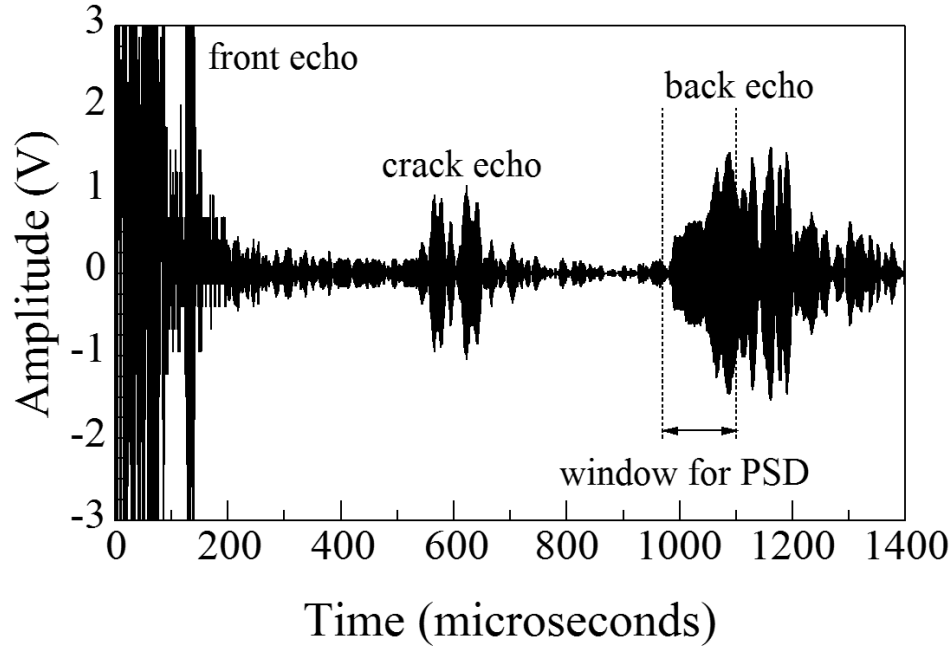

Figure 4. Pulse-Echo Signals Obtained Using Symmetrical Lamb Waves (Narrow Wedge) from Uncoated Plate

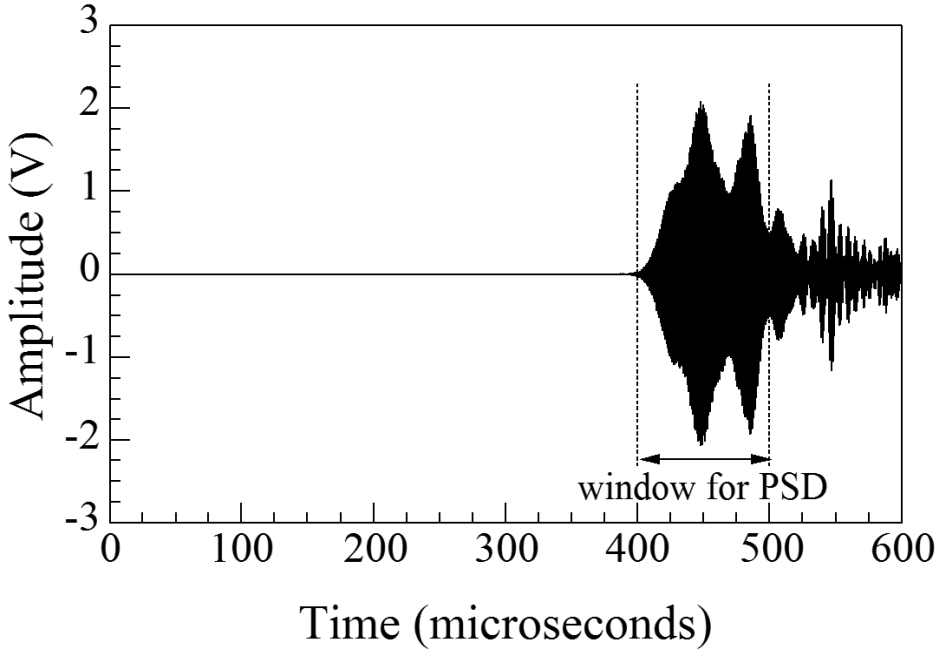

Figure 5. Direct-Transmission Signals Obtained Using Symmetrical Lamb Waves (Broad Wedge) from Uncracked Rusted Plate

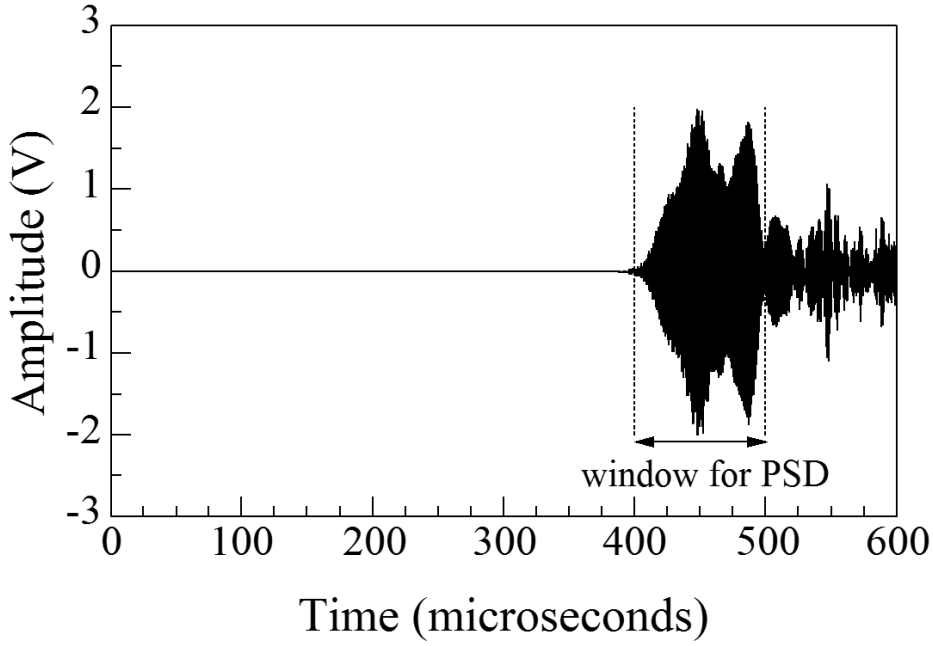

Figure 6. Direct-Transmission Signals Obtained Using Symmetrical Lamb Waves (Broad Wedge) from Cracked Rusted Plate

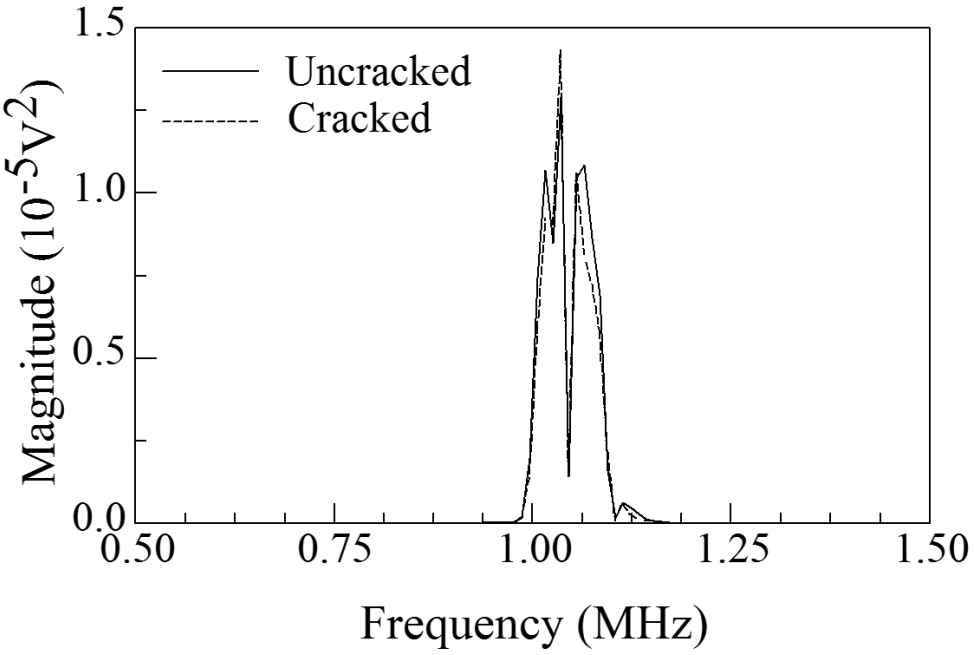

Figure 7. PSD Plots for the Direct-Transmission Signals Shown in Figures 5 and 6

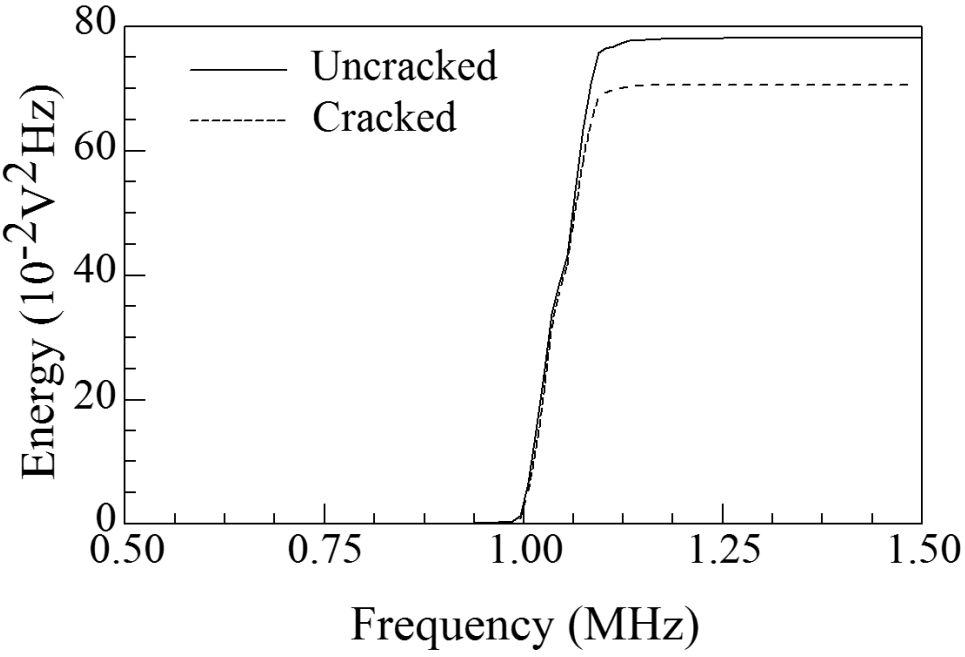

Figure 8. Cumulative Plot for the PSD Curves Shown in Figure 7

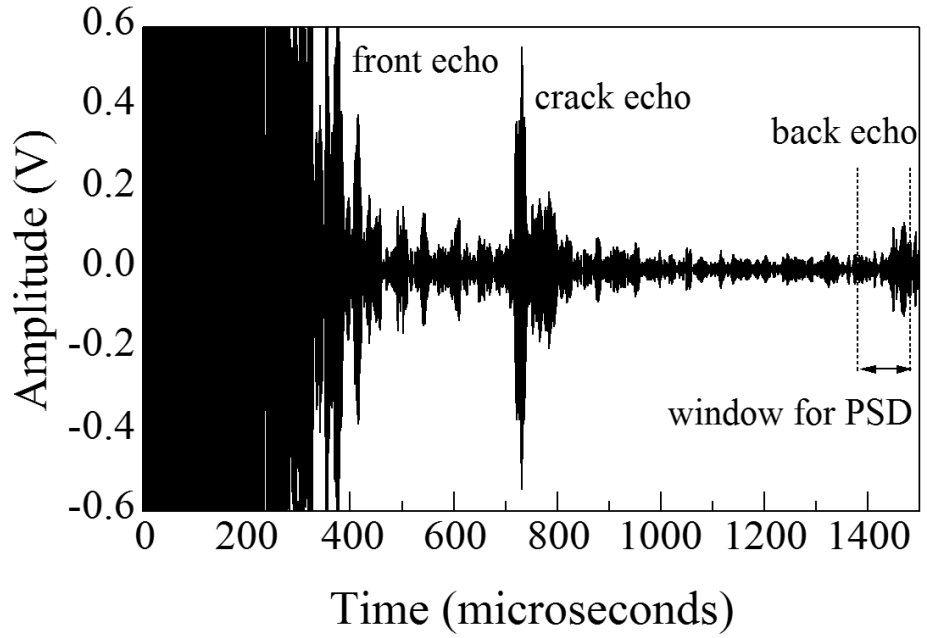

Figure 9. Pulse-Echo Signals Obtained Using Unsymmetrical Lamb Waves from Rusted Plate

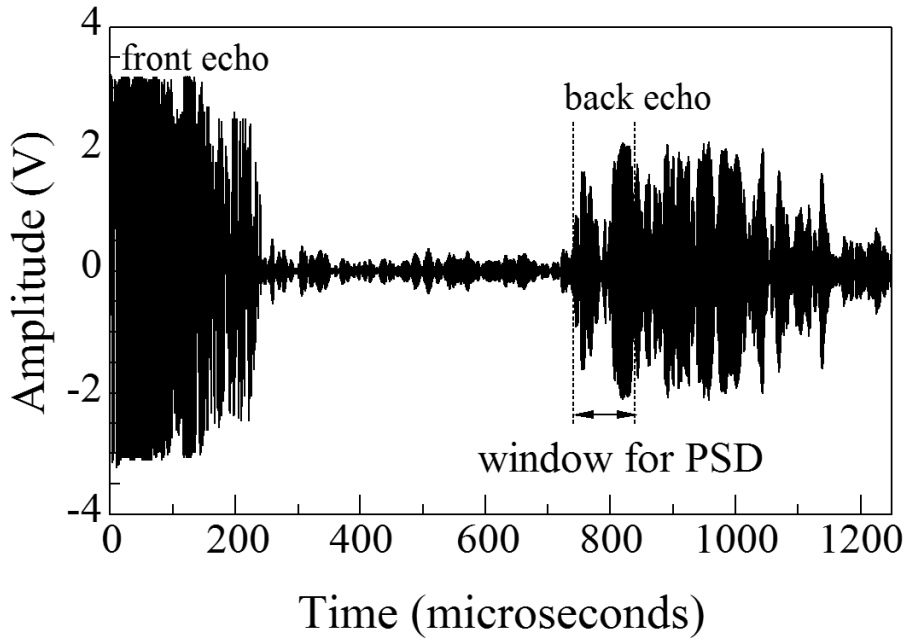

Figure 10. Pulse-Echo Signals Obtained Using Critically Refracted Longitudinal Waves from Uncoated Plate

Table 1. Experimental Results obtained Using Rayleigh Waves

Transmission Mode	Coating	Section	Arrival Time (μs)	Peak-to-Peak Amplitude (V)	Parameters in PSD Curve			
					Peak Magnitude (V^2)	Area (V^2Hz)	Third Moment (V^2Hz^4)	Central Freq. (MHz)
Pulse Echo	Uncoated	Uncracked	1344.4	3.28	2.25×10^{-6}	184.96×10^{-3}	1.44×10^{17}	0.92
		Cracked	1344.3	2.88	9.55×10^{-7}	80.95×10^{-3}	6.54×10^{16}	0.93
	Painted	Uncracked	1408.2	0.09	2.98×10^{-9}	19.79×10^{-5}	1.46×10^{14}	0.90
		Cracked	1406.3	0.06	1.70×10^{-9}	10.77×10^{-5}	7.91×10^{13}	0.86
	Rusted	Uncracked	1382.6	1.02	2.51×10^{-7}	16.96×10^{-3}	1.83×10^{16}	1.01
		Cracked	1384.3	0.64	7.90×10^{-8}	7.10×10^{-3}	6.30×10^{15}	0.96
Direct Transmission	Uncoated	Uncracked	669.6	7.16	1.53×10^{-5}	78.32×10^{-2}	7.67×10^{17}	0.99
		Cracked	676.6	6.00	0.57×10^{-5}	34.03×10^{-2}	3.16×10^{17}	0.97
	Painted	Uncracked	672.5	0.72	6.21×10^{-8}	5.16×10^{-3}	4.66×10^{15}	0.96
		Cracked	682.7	0.12	1.57×10^{-9}	1.26×10^{-4}	1.21×10^{14}	0.98
	Rusted	Uncracked	675.2	5.20	5.93×10^{-6}	42.18×10^{-2}	3.73×10^{17}	0.96
		Cracked	680.2	2.74	1.92×10^{-6}	15.14×10^{-2}	1.36×10^{17}	0.96

Table 2. Experimental Results obtained Using Symmetrical Lamb Waves Generated Using Broad Wedges

Transmission Mode	Coating	Section	Arrival Time (μs)	Peak-to-Peak Amplitude (V)	Parameters in PSD Curve			
					Peak Magnitude (V^2)	Area (V^2Hz)	Third Moment (V^2Hz^4)	Central Freq. (MHz)
Pulse Echo	Uncoated	Uncracked	844.6	1.34	2.95×10^{-6}	10.99×10^{-2}	1.08×10^{17}	1.03
		Cracked	841.3	1.08	1.46×10^{-6}	5.57×10^{-2}	6.04×10^{16}	1.03
	Painted	Uncracked	* *	* *	* *	* *	* *	* *
		Cracked	* *	* *	* *	* *	* *	* *
	Rusted	Uncracked	856.7	1.40	2.56×10^{-6}	8.60×10^{-2}	1.06×10^{17}	1.05
		Cracked	856.9	0.92	9.91×10^{-7}	3.62×10^{-2}	4.46×10^{16}	1.05
Direct Transmission	Uncoated	Uncracked	390.0	5.44	2.02×10^{-5}	106.83×10^{-2}	1.23×10^{18}	1.05
		Cracked	391.8	4.96	1.69×10^{-5}	96.19×10^{-2}	1.12×10^{18}	1.05
	Painted	Uncracked	407.3	0.40	1.40×10^{-7}	8.16×10^{-3}	8.67×10^{15}	1.02
		Cracked	410.8	0.08	3.56×10^{-9}	2.03×10^{-4}	2.09×10^{14}	1.01
	Rusted	Uncracked	398.0	4.16	1.29×10^{-5}	78.71×10^{-2}	9.00×10^{17}	1.05
		Cracked	399.1	3.98	1.44×10^{-5}	70.71×10^{-2}	8.10×10^{17}	1.05

* * Signal echo not seen

Table 3. Experimental Results obtained Using Symmetrical Lamb Waves Generated Using Narrow Wedges

Transmission Mode	Coating	Section	Arrival Time (μs)	Peak-to-Peak Amplitude (V)	Parameters in PSD Curve			
					Peak Magnitude (V^2)	Area (V^2Hz)	Third Moment (V^2Hz^4)	Central Freq. (MHz)
Pulse Echo	Uncoated	Uncracked	871.9	4.44	2.36×10^{-5}	83.27×10^{-2}	9.38×10^{17}	1.05
		Cracked	870.4	2.70	1.01×10^{-5}	39.45×10^{-2}	4.33×10^{17}	1.04
	Painted	Uncracked	* *	* *	* *	* *	* *	* *
		Cracked	* *	* *	* *	* *	* *	* *
	Rusted	Uncracked	873.6	3.60	1.03×10^{-5}	61.43×10^{-2}	7.24×10^{17}	1.05
		Cracked	873.9	2.66	1.04×10^{-5}	29.89×10^{-2}	3.40×10^{17}	1.04
Direct Transmission	Uncoated	Uncracked	398.2	5.54	3.41×10^{-5}	192.30×10^{-2}	2.11×10^{18}	1.05
		Cracked	402.4	6.04	3.16×10^{-5}	156.13×10^{-2}	1.70×10^{18}	1.05
	Painted	Uncracked	415.4	1.22	2.07×10^{-6}	8.64×10^{-2}	9.08×10^{16}	1.02
		Cracked	418.3	0.54	2.29×10^{-7}	1.20×10^{-2}	1.21×10^{16}	1.00
	Rusted	Uncracked	402.4	5.26	3.22×10^{-5}	128.59×10^{-2}	1.49×10^{18}	1.05
		Cracked	405.4	5.06	3.29×10^{-5}	110.50×10^{-2}	1.27×10^{18}	1.05

* * Signal echo not seen

Table 4. Experimental Results obtained Using Unsymmetrical Lamb Waves

Transmission Mode	Coating	Section	Arrival Time (μs)	Peak-to-Peak Amplitude (V)	Parameters in PSD Curve			
					Peak Magnitude (V^2)	Area (V^2Hz)	Third Moment (V^2Hz^4)	Central Freq. (MHz)
Pulse Echo	Uncoated	Uncracked	1389.3	0.76	3.68×10^{-7}	1.70×10^{-2}	1.21×10^{16}	0.90
		Cracked	1390.4	0.46	2.49×10^{-7}	8.96×10^{-3}	6.75×10^{15}	0.91
	Painted	Uncracked	* *	* *	* *	* *	* *	* *
		Cracked	* *	* *	* *	* *	* *	* *
	Rusted	Uncracked	1391.2	0.50	6.18×10^{-8}	3.76×10^{-3}	3.68×10^{15}	0.98
		Cracked	1393.2	0.22	1.98×10^{-8}	1.38×10^{-3}	1.23×10^{15}	0.93
Direct Transmission	Uncoated	Uncracked	661.4	4.28	2.54×10^{-6}	21.41×10^{-2}	1.68×10^{17}	0.92
		Cracked	665.2	4.24	2.07×10^{-6}	19.82×10^{-2}	1.62×10^{17}	0.94
	Painted	Uncracked	671.8	0.34	1.98×10^{-8}	1.41×10^{-3}	1.10×10^{15}	0.91
		Cracked	676.7	0.06	2.85×10^{-10}	2.31×10^{-5}	2.50×10^{13}	1.01
	Rusted	Uncracked	669.2	3.02	1.01×10^{-6}	10.42×10^{-2}	9.75×10^{16}	0.98
		Cracked	674.7	2.02	7.46×10^{-7}	4.77×10^{-2}	4.74×10^{16}	1.00

* * Signal echo not seen

Table 5. Experimental Results obtained Using Critically Refracted Longitudinal Waves

Transmission Mode	Coating	Section	Arrival Time (μs)	Peak-to-Peak Amplitude (V)	Parameters in PSD Curve			
					Peak Magnitude (V^2)	Area (V^2Hz)	Third Moment (V^2Hz^4)	Central Freq. (MHz)
Pulse Echo	Uncoated	Uncracked	705.2	4.82	4.46×10^{-5}	131.63×10^{-2}	13.61×10^{17}	1.01
		Cracked	706.3	4.20	2.63×10^{-5}	93.45×10^{-2}	9.64×10^{17}	1.01
	Painted	Uncracked	711.1	3.32	6.19×10^{-6}	29.33×10^{-2}	3.11×10^{17}	1.01
		Cracked	711.0	2.34	2.54×10^{-6}	14.17×10^{-2}	1.49×10^{17}	1.01
	Rusted	Uncracked	706.3	4.50	2.82×10^{-5}	113.04×10^{-2}	12.22×10^{17}	1.01
		Cracked	707.5	3.46	1.59×10^{-5}	47.38×10^{-2}	5.11×10^{17}	1.01
Direct Transmission	Uncoated	Uncracked	346.4	8.44	10.80×10^{-5}	384.52×10^{-2}	3.97×10^{18}	1.00
		Cracked	347.4	7.52	4.69×10^{-5}	208.75×10^{-2}	2.15×10^{18}	1.00
	Painted	Uncracked	348.2	6.98	5.27×10^{-5}	225.73×10^{-2}	2.29×10^{18}	1.00
		Cracked	348.4	5.10	4.94×10^{-5}	179.18×10^{-2}	1.83×10^{18}	1.00
	Rusted	Uncracked	346.4	7.22	5.94×10^{-5}	263.79×10^{-2}	2.69×10^{18}	1.00
		Cracked	347.2	6.08	3.35×10^{-5}	160.47×10^{-2}	1.62×10^{18}	1.00

Table 6. Attenuation Coefficients

Wave Type	Coating	Attenuation Coefficient, α (m^{-1})	Initial Energy, E_o (V^2Hz)	Coefficient of Determination , R^2
Rayleigh Waves	Unpainted	2.240	11.47	0.998
	Painted	2.642	0.79	0.997
Symmetrical Lamb Waves from Broad Wedges	Unpainted	1.280	0.82	0.997
	Painted	1.650	0.05	0.999
Symmetrical Lamb Waves from Narrow Wedges	Unpainted	1.815	1.01	0.958
	Painted	2.285	0.06	0.952
Unsymmetrical Lamb Waves	Unpainted	1.731	0.02	0.996
	Painted	2.198	0.002	0.999
Critically Refracted Longitudinal Waves	Unpainted	0.850	0.06	0.978
	Painted	0.892	0.02	0.966